Thin Solid Films 780 (2023) 139958

Contents lists available at ScienceDirect

Thin Solid Films

journal homepage: www.elsevier.com/locate/tsf

Al, Mg Co-doped ZnO thin films: Effect of the annealing temperature on the resistivity and ultraviolet photoconductivity

Arpita Das [a], Alakananda Das [a], Chirantan Singha [b], Anirban Bhattacharyya [a,*]

[a] Institute of Radio Physics and Electronics, University of Calcutta, Kolkata 700009, India
[b] Centre for Research in Nanoscience and Nanotechnology, University of Calcutta, Kolkata 700106, India

ARTICLE INFO

Keywords:
Zinc oxide thin film
Sol-gel
Co-doping
Annealing temperature
Photocurrent

ABSTRACT

Interesting electrical and optical properties can be obtained from sol-gel doped Zinc Oxide (ZnO) materials by controlled introduction of dopants in the precursor solution. In this work we investigate the effects of annealing temperature on Al and Mg co-doped ZnO thin films. All samples were dip coated from the same solution, using identical techniques and pre-heating temperature, but were annealed in air at various temperatures ranging from 500°C to 650°C. A three-order magnitude reduction in electrical resistivity was achieved for an increase of 100°C annealing temperature. The structural properties and the energy band-gap remained relatively unchanged during this process. Photocurrent measurements carried out using an ultraviolet excitation source indicate a 5x increase in magnitude, along with increase in persistence behavior. The mechanism behind these effects has been linked to temperature-induced variation in Mg to Al ratio in the films, measured using energy dispersive spectroscopy. Our results indicate that strong in-plane variation of resistivity in ZnO thin films can be carried out using localized heating, opening the way to simpler fabrication processes.

1. Introduction

Zinc Oxide (ZnO) is an important group II-VI semiconductor with attractive electronic and optoelectronic properties. High electron mobility, high thermal conductivity, wide and direct band gap (~3.25 eV) and large exciton binding energy (60 meV) make ZnO suitable for a wide range of optoelectronic, field-emission and MEMS devices [1–4].

In order to develop heterojunction electronic devices, doping and alloying of ZnO materials must be carried out [5]. Alloying of ZnO with small amounts of MgO leads to an increase in the band gap [6]. As the ionic radii of Mg^{2+} and Zn^{2+} are nearly equal, this results in very little lattice distortion. Challenges arise due to the difference in the crystal structures between ZnO (wurtzite) and MgO (rock-salt) which limit the alloy range and related band-gap tunability [7]. On the other hand, Al-doped ZnO (AZO) films have a significant application as Transparent Conductive Oxides (TCO) used in solar cells, liquid crystal displays, heat mirrors, gas sensors, optical position sensors and acoustic wave transducers, making it a good alternative to the more commonly used Indium Tin Oxide (ITO) [8]. Recently doping and co-doping studies on ZnO has been carried out using various elements to either achieve p-type conductivity (N, In) [9,10], for spintronics applications (Mn, Co) [11] or to improve electrical and optical properties in ZnO (Ga, Al Sn, In etc) [12–17].

While sol-gel is a relatively simple low-cost technique, the process allows effective doping of ZnO thin films with various elements by introducing their salts into the precursor solution. Several researchers studied the effect of higher annealing temperature during sol-gel fabrication of Zinc Oxide thin film either doped or co-doped conditions [18–20]. If annealing temperature gradually varied from 450°C to 800°C, the deposited ZnO thin film improved structurally, optically and electrically [21–23]. In addition to these incorporated elements acting as dopants, or modifying the energy band-gap; the improvement of the materials properties may be brought about by other complex mechanisms. These include the modification of grain size and size distribution during growth [24]; incorporation of impurities selectively at grain boundaries thereby affecting current transport and photoconductivity decay [25], and modification of binding energies which in turn effects point defect formation, such as zinc or oxygen vacancies, anti-site defects [26–28], etc.

In our work ZnO thin films have been deposited on soda lime glass substrate using sol-gel. During the deposition of the ZnO thin films, the dip-coated samples were initially baked at 300ºC before a final

* Corresponding author.
E-mail address: anirban1@gmail.com (A. Bhattacharyya).

https://doi.org/10.1016/j.tsf.2023.139958
Received 6 November 2022; Received in revised form 30 May 2023; Accepted 22 June 2023
Available online 25 June 2023

annealing step in air. This final annealing temperature was varied between 500ºC and 650ºC, while maintaining all other parameters the same. We report on the anomalous variation of resistivity with annealing temperature, and discuss the possible mechanism for the same.

2. Experimental details

Sol-gel technique was employed to growth thin films of ZnO on soda-lime glass substrates. Zinc acetate dihydrate ($Zn(CH_3COO)_2.2H_2O$) was dissolved in Isopropanol to form a 0.5 M solution. Subsequently, Diethanolamine ($HN(CH_2CH_2OH)_2$) was added to act as a stabilizer keeping 1:1 ratio with ($Zn(CH_3COO)_2.2H_2O$). The solution was stirred at 60°C for 2 h. For Al/Mg co-doping purpose, Magnesium acetate tetrahydrate [$Mg(CH_3COO)_2.4H_2O$], and Aluminum nitrate nonahydrate ($Al(NO_3)_3{\cdot}9H_2O$) were added, respectively. A precursor solution was prepared with Al/Zn and Mg/Zn atomic ratio of 0.03 and 0.01, respectively [29]. A series of samples are prepared by dip coating 25 mm x 20 mm soda lime glass substrates in the precursor solution, using a vertical motion at a rate of 1 cm/min for insertion and withdrawal, and heated at 300°C for 10 min in air. This process was repeated thrice to generate the desired thickness. During the final heat treatment process, four samples were heated at 500ºC, 550ºC, 600ºC and 650ºC for 30 min to produce co-doped ZnO thin films (measured thickness ~ 100 nm), and the details are given in Table 1.

XRD measurements were carried out using a Rigaku SmartLab (9KW) rotating anode system using the copper Kα line, in the ω-2θ configuration. For optical characterization purpose, optical transmission was carried out using an Ocean Optics Jaz Spectrometer. Photoluminescence spectroscopy was carried out using a He-Cd laser as an excitation source. The surface morphology and the content of Al/Mg in the ZnO thin films were determined by optical microscopy, SEM (Scanning Electron Microscopy) and EDS (Energy-dispersive X-ray Spectroscopy) mounted on a Zeiss EVO 18 scanning electron microscope. UV photo response and persistent photocurrent measurements were conducted using a Keithley 236 Source Measure Unit and mercury lamp. Silver was used as the metal for the formation of Ohmic contacts [30]. Colloidal silver liquid was deposited on the samples as dots of 1mm dimension, then heated on a hot-plate to remove the solvent.

3. Results and discussion

3.1. Resistivity measurements

The samples were investigated by a number of characterization methods in order to determine their structural, electrical and optical properties. Since the rationale for this work was the development of materials for electronic and opto-electronic device applications, electrical properties find prominence in this work. It should be noted that a series of publications have clearly established that the incorporation of Al in ZnO materials lead to a strong reduction of electrical resistivity. Relatively fewer works have been carried out on Mg doping in ZnO, but reports have indicated that such doping can lead to a reduction of electrical conductivity. This has been variously attributed to an overall increase in the energy band gap, thereby reducing dopant ionization probability, or to the presence of very strong Mg-O bond, which reduces the probability of oxygen vacancy formation [31–33], or transport of oxygen through the material grain boundaries. This has been established by previous studies on oxygen out-diffusion during ultraviolet photo-induced current measurements under vacuum conditions. This process is significant for Al-doped ZnO films, but is inhibited when Mg is added as a dopant [34]

Electrical contact formation was carried out using colloidal silver (Pelco TM) in the form of electrodes, whose geometry is shown in the inset of Fig. 1(b). The current-voltage characteristics are presented in Fig. 1(a), and it demonstrates that the contacts are nearly Ohmic in nature with a small degree of saturation at higher voltages, as observed from the deviation from a straight line (dashed).

The resistance of the various samples is plotted together in Fig. 1(b). It should be noted that these films were grown from the same precursor solution under identical coating schemes, except for the final high temperature anneal, which was carried out at different temperatures. It is therefore very interesting to note that variation of annealing temperature from 500°C to 550°C reduces the resistance of the sample by more than two orders or magnitude. The resistance decreased by another order in magnitude from 500°C to 600°C, before increasing for higher annealing temperature of 650°C.

Table 1
Details of samples studied.

Sample No.	Al/Zn, Mg/Zn atomic ratio in solution	Substrate temperature
S_500	0.03, 0.01	500ºC
S_550	0.03, 0.01	550ºC
S_600	0.03, 0.01	600ºC
S_650	0.03, 0.01	650ºC

3.2. X-ray diffraction and scanning electron microscopy

The conductivity of a sample may increase from annealing at higher temperature, either from an increase of mobility, or of carrier concentrations. Increased mobility may occur due to an increase in the size of crystallites, or domains, due to solid-state diffusion during the annealing

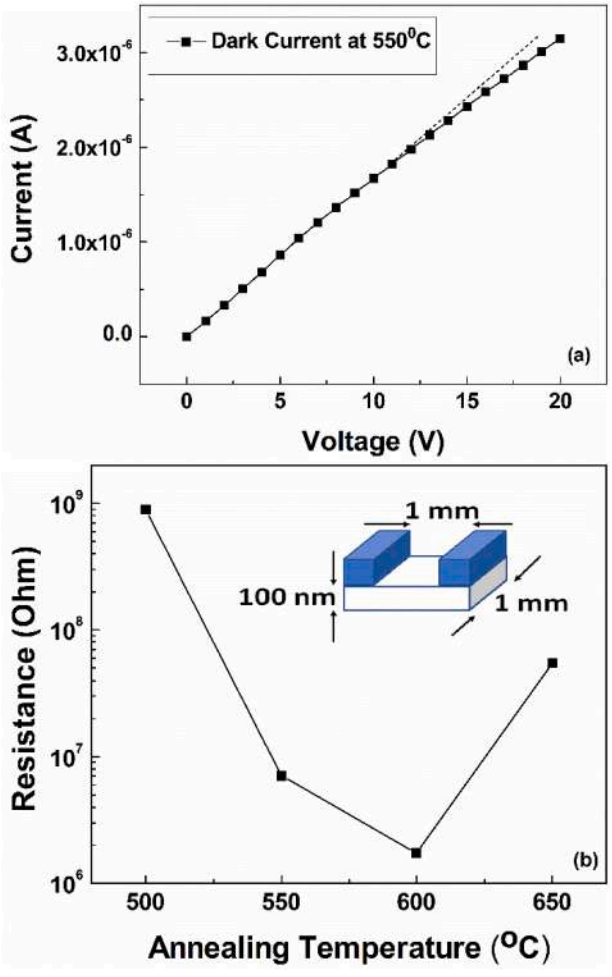

Fig. 1. (a) I-V characteristics for sample S_550, (b) variation of electrical Resistance with annealing temperature for all samples (contact geometry shown in inset).

step. In order to determine if that is applicable in this case, X-ray diffraction measurements were carried out on all four samples, and the results are presented in Fig. 2.

The films investigated were found to be polycrystalline, with the (100), (002) and (101) orientations of ZnO being clearly visible. The peak at ~38° is due to silver contacts, and can be neglected for the purposes of this discussion. The crystallite size has been calculated from the FWHM using the Scherrer's equation [29] and the results are presented below in Table 2. It shows a clear but small increase in the grain size with annealing temperature, which is commonly observed in all such studies. We do not believe that this has much significance in explanation of the phenomena described in the paper.

It can be clearly understood that while the relative magnitudes of the peaks from various crystal orientations, which corresponds to the proportion of oriented crystallites in the film, is somewhat different for the four samples, the overall nature of the crystallinity remains the same, and the preferential (002) orientation that has been observed by some groups [35] at higher annealing temperature is not present in this work. There is a similar increase in crystallite size for all orientations, for example from 14 nm to 28 nm for (002) orientation, as the annealing temperature was increased from 500°C to 550°C. However, the change is monotonic with temperature, and is not expected to play a significant role in the complex and order-of-magnitude variation of conductivity, as was observed. The variation of crystallite size is also reflected in the SEM images for samples S_500 and S_650, shown in Fig. 3.

3.3. Optical studies

Studies in the literature indicate that the role of deliberately incorporated impurities in modulating the optical band-gap of semiconductors such as ZnO. For heavily doped AZO (Aluminum Zinc Oxide), the band-gap enlarges due to the Burstein Moss effect [36]. Doping also tends to create band-tails, and the Urbach energy is a measure of the state of disorder in the material [37]. Mg incorporation is expected to enlarge the band-gap [38], but this process is complicated by the large disparity of the crystal symmetry of MgO which is rutile and ZnO which is hexagonal. In order to determine if our primary finding, the orders of magnitude increase in conductivity due to change in annealing temperature is due to variation in band-gap, optical absorption studies were carried out and the four samples are compared in Fig. 4 (a).

The optical transmissions for the samples were measured using spectrophotometry, and the results were used to obtain the absorption coefficient (α) using the simple relationship given below:

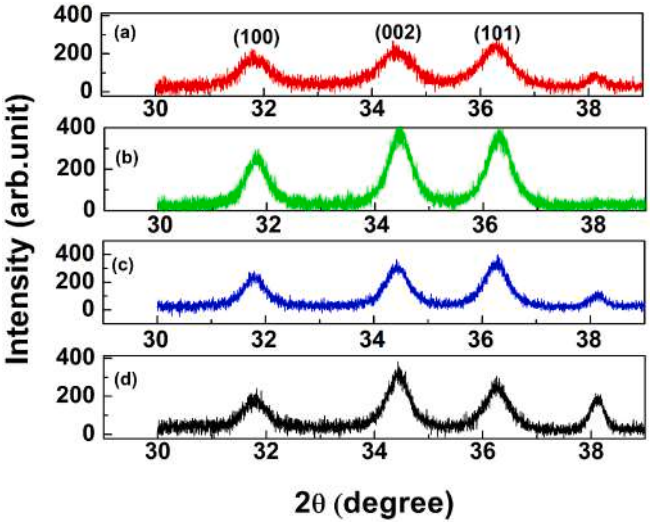

Fig. 2. XRD pattern of the samples (a) S_500 (b) S_550 (c) S_600 and (d) S_650.

$$I = I_o \exp(-\alpha.d) \quad (1)$$

where I_o and I are the incident and transmitted light respectively, and d is the thickness of the sample.

From Fig. 4(a) it is clear that the four samples have a very similar nature, except for a more prominent peak, which can be attributed to excitonic transitions, observed for sample annealed at the highest temperature. The energy band-gap was estimated by the peak of the derivative $d\alpha/dE$ where E is the photon energy, when plotted against E [39], as shown in the inset of Fig. 4(a). The values of the energy band-gaps found by this method show that the band-gap has a decreasing trend with annealing temperature, but the effect is quite weak and very close to the limits of experimental error (Fig. 4(b)).

The same plot also shows the variation of the Urbach energy [40–43] for the four samples on the right axis. It can be observed that the Urbach energy is higher for the sample annealed at 550°C, even though the values are not widely disparate.

Photoluminescence spectroscopy was carried out at room temperature, using a 325 nm laser with low intensity as an excitation source. In Fig. 5(a), the decay from the scattering of the laser tail can be clearly observed for wavelengths shorter than 350 nm. All samples show a clear single band-edge peak around 380 nm, which is indicative of their overall quality. It should be noted that the features around 500 nm are an artefact of measurement, arising from the laser itself, and therefore are not part of the discussion. The absence of a green luminescence arising from the samples indicates that surface states do not play a significant role. There is however a strong longer wavelength tail, which extends till 500 nm.

The photoluminescence spectrum for each of the samples show a single near band-edge (NBE) peak at ~380 nm, along with a long-wavelength tail that spans the wavelength range 400 nm to nearly 500 nm. Detailed analysis indicates the presence of multiple overlapping peaks within this tail, with progressively diminishing amplitudes. It is likely that these peaks are generated due to transitions from donor states near the conduction band, or are linked to donor-bound excitons, along with their phonon replica [44,45]. Detailed analysis is beyond the scope of this paper and will be published elsewhere. It can however be stated qualitatively that similar features are observed for all the spectra, irrespective of the annealing temperature, except for the variation in intensity, which is shown in Fig. 5(b). The PL intensity progressively increases for samples annealed at higher temperatures, before reducing somewhat for sample annealed at 650°C. This dependence qualitatively replicates that of the electrical conductivity, and causality is likely to exist. It has been observed in many semiconductors, especially those with large defect densities that the photoluminescence intensity increases with free carrier concentration. This has been attributed to compensation of defect states by these carriers, typically free electrons, which otherwise would act as non-radiative recombination centers.

3.4. Energy dispersive spectroscopy (EDS)

From the structural and optical characterization results, it is clear that there are no fundamental changes observed with annealing temperature that can even qualitatively explain the orders-of-magnitude change in conductivity with annealing temperature increasing from 500°C to 600°C. This indicates that the change is essentially from carrier concentration, rather than mobility. Strong variation in carrier concentration can be linked to dopant incorporation, dopant activation, or selective trapping of carriers at defect sites. In order to determine the first component, extensive studies of dopant incorporation into the films were investigated using energy dispersive spectroscopy (EDS). It should be reiterated that the films were all grown from the same precursor solution. As has been stated previously, the Al/Zn and Mg/Zn ratio in the precursor solution was taken to be 0.03 and 0.01, respectively. EDS results on the sample S_500 indicate that the corresponding ratios in the

Table 2
Calculation of FWHM and crystallite size from XRD pattern.

Sample Specification	Along (100) direction		Along (002) direction		Along (101) direction	
	FWHM (Degree)	Crystallite Size (nm)	FWHM (Degree)	Crystallite Size (nm)	FWHM (Degree)	Crystallite Size (nm)
S_500	0.47	17.5	0.57	14.6	0.48	17.5
S_550	0.33	25.3	0.34	24.5	0.34	24.7
S_600	0.32	26.2	0.32	25.9	0.34	24.7
S_650	0.32	26.2	0.30	28	0.32	26.5

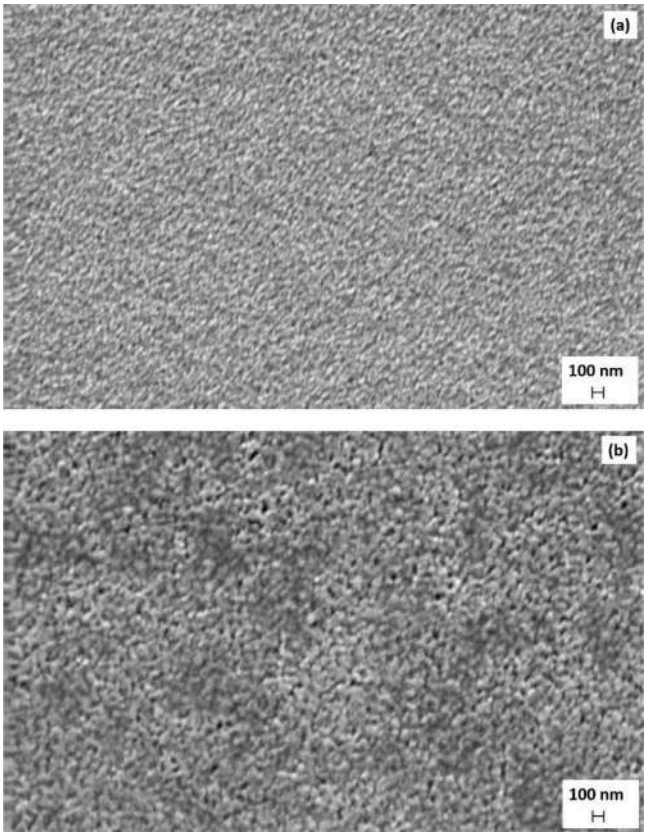

Fig. 3. SEM images for sample (a) S_500 and (b) S_650.

film were found to be 0.023 and 0.013. Such variation has been reported extensively in our previous publication [29].

Since there are a number of unknown parameters that can generate errors in absolute measurements of atomic concentration of elements during EDS measurements, we only report the relative concentrations of Al to Mg, benchmarked to the value measured for the sample annealed at 500°C. This process is expected to cancel out all systematic errors, as only relative values are used in the analysis. The results comparing the four samples annealed at different temperatures are shown in Fig. 6. The Al to Mg ratio increases progressively as the annealing temperature is increased from 500°C to 600°C and then reduces slightly. Two conclusions can be readily drawn from comparison with this figure to the results on resistivity in Fig. 1. Firstly, it is clear that the decrease in resistance, which was shown to be driven by a change in free carrier concentration, can be directly linked to Al doping levels. Secondly, only the Al to Mg dopant concentration ratio cannot account for all aspects of the resistance change.

Specifically, the increase in Al to Mg ratio is smaller when the annealing temperature is increased from 500°C to 550°C, than when it in increased from 550°C to 600°C. In contrast, the change in resistance is much higher in the first range than the second. In order to further establish the connection between the Al to Mg ratio and the change in

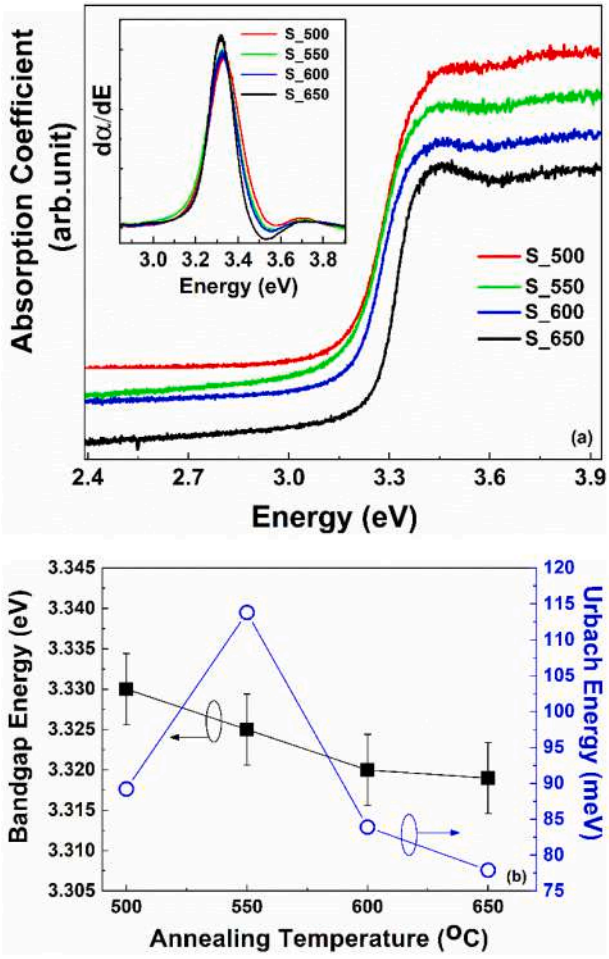

Fig. 4. (a) Optical Absorption spectra for samples S_500, S_550, S_600 and S_650 (b) Variation of Energy Band-gap and Urbach energy with annealing temperature.

resistance, a second series of samples were grown under slightly changed conditions of precursor solution and coating schemes, and qualitatively similar results were obtained, as shown in Fig. 6. For both the series of samples, the Al to Mg ratio qualitatively reflects the variation of electrical resistance.

In order to further investigation, the effect of annealing temperature on the electrical properties of the samples, ultraviolet photoconduction measurements were carried out on the first series of samples, and the results are shown in Fig. 7. A Mercury lamp was used as an excitation source. Fig. 7(a) shows the I-V characteristics for the samples under illumination. The weakest photocurrent levels occur for sample annealed at 500°C, which increases progressively for samples annealed at 550°C and 600°C, before reducing sharply. The decay of photocurrent transients was measured for the four samples, under different voltage bias (Fig. 7(b)). Persistent photocurrent is strong for all four samples, even though the decays were faster for higher bias voltages. However, it

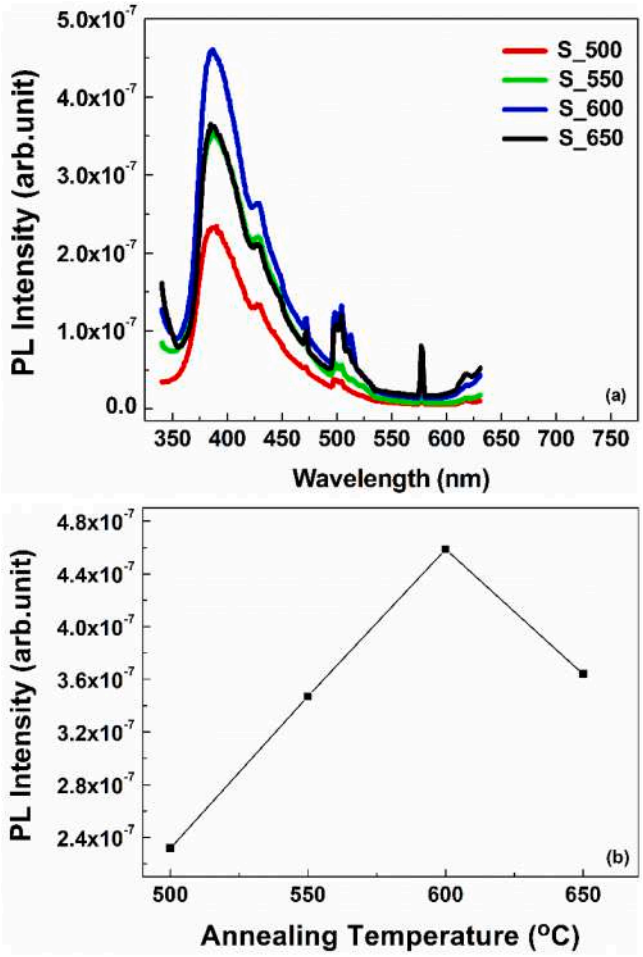

Fig. 5. (a) Room Temperature Photoluminescence (RT-PL) spectrum and (b) variation of NBE PL peak with annealing temperature for samples S_500, S_550, S_600 and S_650.

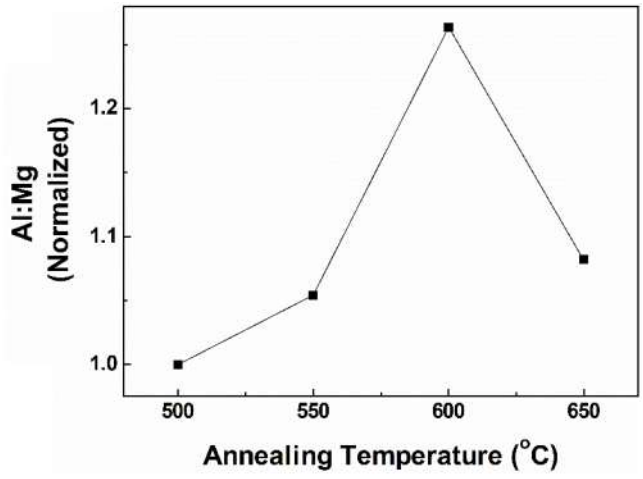

Fig. 6. Variation of Al/Mg atomic ratio measured by EDS, normalized against the sample S_500.

should be pointed out that the decay times were slowest for the sample annealed at 600°C, which also showed the highest photocurrent values. This is consistent with the presence of single or multiple defect states that act as trapping centers for one of the carriers, either electrons or holes. The trapping enhances the carrier lifetimes, and the photocurrent

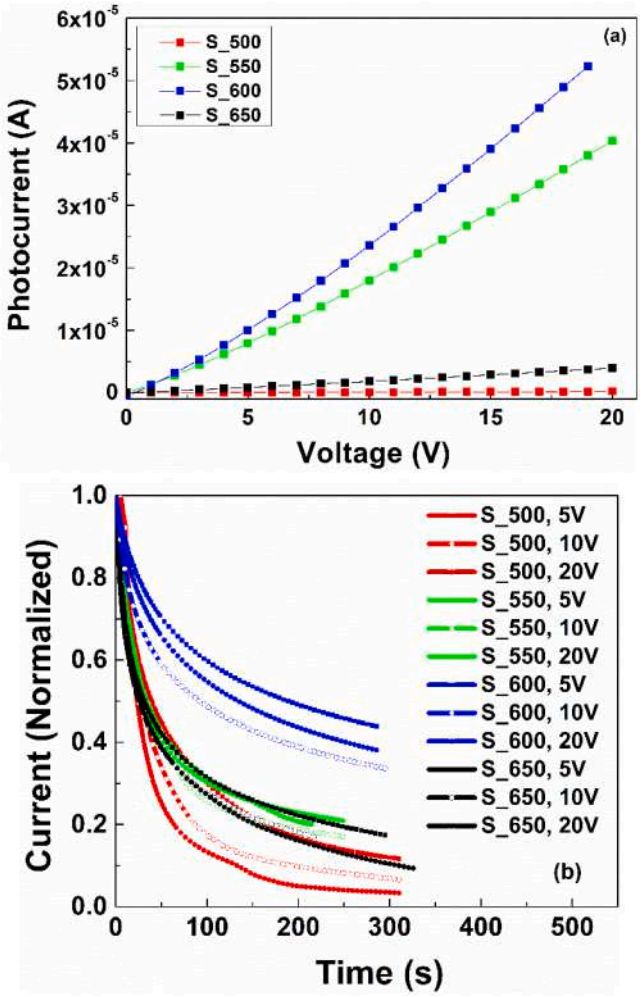

Fig. 7. (a) Photocurrent vs. Voltage plot and (b) photocurrent transient decay measured at 5,10 and 20V bias for samples S_500, S_550, S_600 and S_650.

levels in the material. Since Al has been linked in previous work by our group [29], to the presence of trap levels and long persistent photocurrent lifetimes, it is clear that the photocurrent results can also be linked to the Al to Mg ratio as measured by EDS.

From the above discussion, we can directly link the electrical and optical properties of ZnO co-doped thin films to the ratio of Al to Mg incorporated in the film, as determined by EDS. However, the physical processes that link this ratio to the annealing temperature of the thin films remains to be addressed. While it is difficult to pinpoint exact mechanism, it can be safely assumed that since the samples were grown from the same precursor solution, the determining factor was the relative evaporation rate of Al and Mg. Since Mg has a much higher vapor pressure than Al, increasing the annealing temperature would preferentially evaporate Mg over Al. However, we are unable to address why this ratio move the other direction at 650°C. It may be related to the melting point of Al, which is 635°C, but it is difficult to comment on the mechanism.

4. Conclusions

In this paper we demonstrate the strong variation of electrical conductivity with annealing temperature for sol-gel grown ZnO co-doped with Al and Zn. A 50°C increase in annealing temperature was shown to increase the conductivity of the film by more than two orders in magnitude. This result was not due to a change in the structural properties of the material, but was linked to the variation of Al to Mg ratio

within the film, which was found to increase with annealing temperature.

Our results indicate a simpler path for development of electrical and optoelectronic devices based on sol-gel grown ZnO thin film. Deliberate in-plane variation of electrical conductivity can be carried out using a laser, operating in the raster-scan mode, which can generate localized heating. This will be an affordable alternative process, as only a small change in annealing temperature can cause orders of magnitude change in conductivity. This method can be used in development of isolation pads, interconnects, etc, using localized laser heating, without the need for expensive and complex lithography-based doping-related device fabrication steps.

CRediT authorship contribution statement

Arpita Das: Conceptualization, Methodology, Writing – review & editing, Supervision. **Alakananda Das:** Investigation, Validation, Writing – original draft, Visualization. **Chirantan Singha:** Investigation, Validation. **Anirban Bhattacharyya:** Investigation, Validation.

Declaration of Competing Interest

The authors declare that they have no known competing financial interests or personal relationships that could have appeared to influence the work reported in this paper.

Data availability

Data will be made available on request.

Acknowledgment

The author, Arpita Das is currently at University of Engineering and Management, Kolkata (Department: Electronics and Communication Engineering), and this research work was completed during her doctoral studies at University of Calcutta.The authors would like to acknowledge Center for Research in Nanoscience and Nanotechnology (CRNN), University of Calcutta for XRD measurements. Alakananda Das would like to acknowledge the Council of Scientific and Industrial Research Senior Research Fellowship (CSIR-SRF) scheme (09/028(0946)/2015-EMR-I). Chirantan Singha would like to acknowledge the Department of Science and Technology (DST) INSPIRE fellowship (IF120257) for funding his work.

References

[1] A. Janotti, C.G. VandeWalle, Fundamentals of zinc oxide as a semiconductor, Rep. Prog. Phys. 72 (2009), 126501, https://doi.org/10.1088/0034-4885/72/12/126501.
[2] A.K. Radzimska, T. Jesionowski, Zinc oxide—from synthesis to application: a review, Materials 7 (2014) 2833–2881, https://doi.org/10.3390/ma7042833.
[3] U. Ozgur, D. Hofstetter, H. Morkoc, ZnO devices and applications: a review of current status and future prospects, Proc. IEEE 98 (7) (2010) 1255–1268, https://doi.org/10.1109/JPROC.2010.2044550.
[4] B.K. Sonawane, M.P. Bhole, D.S. Patil, Structural, optical and electrical properties of post annealed Mg doped ZnO films for optoelectronics applications, Opt. Quant. Electron 41 (2009) 17–26, https://doi.org/10.1007/s11082-009-9317-y.
[5] S. Nandi, S. Kumar, A. Misra, Zinc oxide heterostructures: advances in devices from self-powered photodetectors to self-charging supercapacitors, Mater. Adv. 2 (2021) 6768–6799, https://doi.org/10.1039/D1MA00670C.
[6] M. Salina, R. Ahmed, A.B. Suriani, M. Rusop, Bandgap alteration of transparent zinc oxide thin film with Mg dopant, Trans. Electr. Electron. Mater. 13 (2012) 64–68, https://doi.org/10.4313/TEEM.2012.13.2.64.
[7] F.K. Shan, B.I. Kim, G.X. Liu, Z.F. Liu, J.Y. Sohn, W.J. Lee, B.C. Shin, Y.S. Yu, Blueshift of near band edge emission in Mg doped ZnO thin films and aging, J. Appl. Phys. 95 (2004) 4772–4776, https://doi.org/10.1063/1.1690091.
[8] M.C Jun, J.H Koh, Optical and structural properties of Al-doped ZnO thin films by sol gel process, J. Nanosci. Nanotechnol. 13 (5) (2013) 3403–3407, https://doi.org/10.1166/jnn.2013.7314.
[9] J.M. Bian, X.M. Li, X.D. Gao, W.D. Yu, L.D. Chen, Deposition and electrical properties of N–In codoped p-type ZnO films by ultrasonic spray pyrolysis, Appl. Phys. Lett. 84 (2004) 541–543, https://doi.org/10.1063/1.1644331.
[10] M. Joseph, T.Kawai H.Tabata, p-Type electrical conduction in ZnO thin films by Ga and N codoping, J. Appl. Phys. 38 (1999) 1205–1207, https://doi.org/10.1143/JJAP.38.L1205.
[11] L. Yan, C.K. Ong, X.S. Rao, Magnetic order in Co-doped and (Mn, Co) codoped ZnO thin films by pulsed laser deposition, J. Appl. Phys. 96 (2004) 508–511, https://doi.org/10.1063/1.1757652.
[12] J. Beckford, M.K. Behera, K. Yarbrough, B. Obasogie, S.K. Pradhan, M. Bahoura, Gallium doped zinc oxide thin films as transparent conducting oxide for thin-film heaters, AIP Adv. 11 (7) (2021), 075208, https://doi.org/10.1063/5.0016367.
[13] X. Jiang, F.L. Wong, M.K. Fung, S.T. Lee, Aluminum-doped zinc oxide films as transparent conductive electrode for organic light-emitting devices, Appl. Phys. Lett. 83 (2003) 1875, https://doi.org/10.1063/1.1605805.
[14] By. Li, Ff. Liu, L. Lin, Sn doped ZnO thin films as high resistivity window layer for $Cu(In,Ga)Se_2$ solar cells, Optoelectron. Lett. 16 (2020) 451–454, https://doi.org/10.1007/s11801-020-0054-6.
[15] S. Major, K.L. Chopra, Indium-doped zinc oxide films as transparent electrodes for solar cells, Solar Energy Mater. 17 (5) (1988) 319–327, https://doi.org/10.1016/0165-1633(88)90014-7.
[16] T. Minami, Transparent conducting oxide semiconductors for transparent electrodes, Semicond. Sci. Technol. 20 (4) (2005), https://doi.org/10.1088/0268-1242/20/4/004.
[17] W.J. Jeong, S.K. Kim, G.C. Park, Preparation and characteristic of ZnO thin film with high and low resistivity for an application of solar cell, Thin. Solid. Films 506–507 (2006) 180–183, https://doi.org/10.1016/j.tsf.2005.08.213.
[18] S.K. Sahoo, C.A. Gupta, U.P. Singh, Impact of Al and Ga co-doping with different proportion in ZnO thin film by DC magnetron sputtering, J. Mater. Sci. Mater. Electron. 27 (2016) 7161–7166, https://doi.org/10.1007/s10854-016-4679-y.
[19] R. Ghosh, G.K. Paul, D. Basak, Effect of thermal annealing treatment on structural, electrical and optical properties of transparent sol–gel ZnO thin films, Mater. Res. Bull. 40 (11) (2005) 1905–1914, https://doi.org/10.1016/j.materresbull.2005.06.010.
[20] A. Goktas, A. Tumbul, Z. Aba, M. Durgun, Mg doping levels and annealing temperature induced structural, optical and electrical properties of highly c-axis oriented ZnO:Mg thin films and Al/ZnO:Mg/p-Si/Al heterojunction diode, Thin. Solid. Films 680 (2019) 20–30, https://doi.org/10.1016/j.tsf.2019.04.024.
[21] F.H. Wang, C.L. Chang, Effect of substrate temperature on transparent conducting Al and F co-doped ZnO thin films prepared by rf magnetron sputtering, Appl. Surf. Sci. 370 (2016) 83–91, https://doi.org/10.1016/j.apsusc.2016.02.161.
[22] M. Jun, J. Koh, Effects of annealing temperature on properties of Al-doped ZnO thin films prepared by sol-gel dip-coating, J. Electr. Eng. Technol. 8 (1) (2013) 163–167, https://doi.org/10.5370/JEET.2013.8.1.163.
[23] D. Raoufi, T. Raoufi, The effect of heat treatment on the physical properties of sol–gel derived ZnO thin films, Appl. Surf. Sci. 255 (11) (2009) 5812–5817, https://doi.org/10.1016/j.apsusc.2009.01.010.
[24] F. Ruske, M. Roczen, K. Lee, M. Wimmer, S. Gall, J. Hupkes, D. Hrunski, B. Rech, Improved electrical transport in Al-doped zinc oxide by thermal treatment, J. Appl. Phys. 107 (1) (2010), https://doi.org/10.1063/1.3269721, 013708(1-8).
[25] Y. Zhang, W. Fa, F. Yang, Z. Zheng, P. Zhang, Effect of annealing temperature on the structural and optical properties of ZnO thin films prepared by sol–gel method, Ionics 16 (2010) 815–820, https://doi.org/10.1007/s11581-010-0468-4.
[26] X.L. Zhang, K.S. Hui, F. Bin, K.N. Hui, L. Li, Y.R. Choa, R.S. Mane, W. Zhou, Effect of thermal annealing on the structural, electrical and optical properties of Al–Ni co-doped ZnO thin films prepared using a sol–gel method, Surf. Coat. Technol. 261 (2015) 149–155, https://doi.org/10.1016/j.surfcoat.2014.11.043.
[27] V.S. Santhosh, K. Rajendra Babu, M. Deepa, Influence of Fe dopant concentration and annealing temperature on the structural and optical properties of ZnO thin films deposited by sol–gel method, J. Mater. Sci. Mater. Electron. 25 (1) (2013) 224–232, https://doi.org/10.1007/s10854-013-1576-5.
[28] D. Fang, P. Yao, H. Li, Influence of annealing temperature on the structural and optical properties of Mg–Al co-doped ZnO thin films prepared via sol–gel method, Ceram. Int. 40 (4) (2014) 5873–5880, https://doi.org/10.1016/j.ceramint.2013.11.030.
[29] A. Das, P.G. Roy, A. Dutta, S. Sen, P. Pramanik, D. Das, A. Banerjee, A. Bhattacharyya, Mg and Al co-doping of ZnO thin films: Effect on ultraviolet photoconductivity, Mater. Sci. Semicond. Process. 54 (2016) 36–41, https://doi.org/10.1016/j.mssp.2016.06.018.
[30] S. Mondal, K. P.Kanta, P. Mitra, Preparation of ZnO film on p-Si and I-V characteristics of p-Si/n-ZnO, Mater. Res. 16 (2013) 94–99, https://doi.org/10.1590/S1516-14392012005000149.
[31] C.J. Ku, Z. Duan, P.I. Reyes, Y. Lu, Yi Xu, C.L. Hsueh, E. Garfunkel, Effects of Mg on the electrical characteristics and thermal stability of $Mg_xZn_{1-x}O$ thin film transistors, Appl. Phys. Lett. 98 (2011), 123511, https://doi.org/10.1063/1.3567533.
[32] X. Yu, X. Yu, M. Yan, T. Weng, L. Chen, Y. Zhou, J. Wei, Lowering oxygen vacancies of ZnO nanorods via Mg-doping and their effect on polymeric diode behavior, Sens. Actuator A Phys. 312 (2020), 112163, https://doi.org/10.1016/j.sna.2020.112163.
[33] L. Cao, L. Zhu, Z. Ye, Enhancement of p-type conduction in Ag-doped ZnO thin films via Mg alloying: the role of oxygen vacancy, J. Phys. Chem. Solids 74 (2013) 668–672, https://doi.org/10.1016/j.jpcs.2012.12.025.
[34] A. Das, P.G. Roy, S. Sen, A. Bhattacharyya, Mg and Al doped ZnO thin film: photoinduced “oxygen breathing” under UV illumination, Thin. Solid. Films 662 (2018) 54–59, https://doi.org/10.1016/j.tsf.2018.07.021.

[35] M. Arif, A. Sanger, P.M. Vilarinho, A. Singh, Effect of annealing temperature on structural and optical properties of Sol–Gel-derived ZnO thin films, J. Electron. Mater. 47 (2018) 3678–3684, https://doi.org/10.1007/s11664-018-6217-6.
[36] C.H. Zhai, R.J. Zhang, X. Chen, Y.X. Zheng, S.Y. Wang, J. Liu, N. Dai, L.Y. Chen, Effects of Al doping on the properties of ZnO thin films deposited by atomic layer deposition, Nanoscale Res. Lett. 11 (2016) 407, https://doi.org/10.1186/s11671-016-1625-0.
[37] R. Vettumperumal, S. Kalyanaraman, B. Santoshkumar, R. Thangavel, Estimation of electron–phonon coupling and Urbach energy in group-I elements doped ZnO nanoparticles and thin films by sol–gel method, Mater. Res. Bull. 77 (2016) 101–110, https://doi.org/10.1016/j.materresbull.2016.01.015.
[38] K. Huang, Z. Tang, L. Zhang, J. Yu, J. Lv, X. Liu, F. Liu, Preparation and characterization of Mg-doped ZnO thin films by sol–gel method, Appl. Surf. Sci. 258 (8) (2012) 3710–3713, https://doi.org/10.1016/j.apsusc.2011.12.011.
[39] A.K. Zak, A.M Hashim, M. Darroudi, Optical properties of ZnO/BaCO3 nanocomposites in UV and visible regions, Nanoscale Res. Lett. 9 (2014) 399, https://doi.org/10.1186/1556-276X-9-399.
[40] S. Chichibu, T. Mizutani, T. Shioda, H. Nakanishi, Urbach–Martienssen tails in a wurtzite GaN epilayer, Appl. Phys. Lett. 70 (25) (1997) 3440, https://doi.org/10.1063/1.119196.
[41] F. Yakuphanoglu, Y. Caglar, S. Ilican, M. Caglar, The effects of fluorine on the structural, surface morphology and optical properties of ZnO thin films, Phys. B Condens. 394 (1) (2007) 86–92, https://doi.org/10.1016/j.physb.2007.02.014.
[42] R.C. Rai, Analysis of the Urbach tails in absorption spectra of undoped ZnO thin films, J. Appl. Phys. 113 (15) (2013), https://doi.org/10.1063/1.4801900, 153508 (1-5).
[43] M. Yilmaz, Investigation of characteristics of ZnO:Ga nanocrystalline thin films with varying dopant content, Mater. Sci. Semicond. Process. 40 (2015) 99–106, https://doi.org/10.1016/j.mssp.2015.06.031.
[44] H. Chen, J. Ding, S. Ma, Structural and optical properties of ZnO:Mg thin films grown under different oxygen partial pressures, Physica E42 (2010) 1487–1491, https://doi.org/10.1016/j.physe.2009.12.005.
[45] X.Q. Wei, Z.G. Zhang, M. Liu, C.S. Chen, G. Sun, C.S. Xue, H.Z. Zhuang, B.Y. Man, Annealing effect on the microstructure and photoluminescence of ZnO thin films, Mater. Chem. Phys. 101 (2007) 285–290, https://doi.org/10.1016/j.matchemphys.2006.05.005.